

## Dynamic Mechanical Behavior of Highly Filled Polymers: Dewetting Effect

A. LEPIE and A. ADICOFF, *Chemistry Division, Polymer Science Branch, Naval Weapons Center, China Lake, California 93555*

### Synopsis

This paper describes the results of simultaneous dynamic measurements in tension and torsion made on propellant samples. The complex dynamic moduli  $E'$ ,  $E''$ ,  $G'$ , and  $G''$  at low frequencies were determined within a temperature range from room temperature to  $-90^{\circ}\text{C}$ . Time temperature shift factors and reduced master curves for both tension and shear properties are discussed. The effect of dewetting on the dynamic properties in tension and shear was also investigated. A preliminary attempt is made to compute the degree of dewetting in a propellant by applying Beer-Lambert's law.

### INTRODUCTION

Mechanical spectroscopy is a tool useful for obtaining information about the mechanical behavior of polymers and for understanding some of the details involved in the microstructure of unfilled and filled systems. The investigations reported in this paper made use of a mechanical oscillator as a spectrometer, which is described in previous publications.<sup>1-3</sup>

Basically this device applies superposed small mechanical oscillations in tension and torsion to a sample before and during the time it is subjected to finite uniaxial strains. From the data obtained, one can determine both dynamic loss and storage moduli in tension and shear while simultaneously recording the finite stresses in the sample as functions of strain and relaxation time.

The apparatus is a combined torsion-tension tester which is built into an Instron machine and designed in such a manner as to enable the sample to be axially elongated by driving the Instron cross head down. The sample, which is suspended from a piano wire, can be twisted under strain.

As, or after, the sample is axially strained, it is subjected either simultaneously or alternately to superposed oscillations in tension and torsion with adjustable amplitudes of 0 to  $\pm 0.3$  cm or 0 to  $\pm 6$  degrees, respectively. The load responses are measured using a 100-kg Instron load cell (CTM) in tension and Photocon transducers with 0 to 1-pound and 0 to 10-pound ranges in torsion ( $\pm 0.1$  g). Frequencies can be precisely achieved in a number of discrete steps from 0.005 to 5 Hz. Displacements of the samples are recorded via DCDTs ( $\pm 0.001$  cm). At frequencies of 1 Hz or

lower, the data are recorded as stress-strain hysteresis on a Moseley x-y recorder which has an accuracy of 0.2% at full scale.

Loss tangents and dynamic forces in torsion and tension were determined from hysteresis loops. Phase shift corrections for the Instron load cell were considered. No phase shift was observed for the DCDTs within this low frequency range.

Dynamic tests on linear viscoelastic samples result in characteristic complex moduli as functions of frequency and temperature. The amplitude employed in the dynamic tests is an additional important parameter for nonlinear viscoelastic characterization.

If one considers dynamic losses in mechanical spectroscopy as one considers absorbances in optical spectroscopy, the techniques of optical spectroscopy can be applied to determine concentrations of functional groupings contributing to the dynamic loss transitions. A preliminary attempt is made in this paper to compute the extent of dewetting in a propellant, applying Beer-Lambert's law.

## EXPERIMENTAL

The propellant samples used for the experiments were rectangular specimens of size  $7 \times 1 \times 1$  cm. A description of the dynamic measurement method and the apparatus was published in detail previously.<sup>3</sup>

The measurements reported in this paper were performed after returning the sample to the zero stress state. The temperature control of the sample was maintained using a Data-Trak programmer with thermal controller and a specially designed cyclonic air bath utilizing, below room temperature, a liquid nitrogen injection mechanism. The thermal gradients in the sample chamber were less than 1°C from the indicated values.

The changes in the samples' thickness were measured by means of a newly developed caliper employing a linear variable differential transformer. The propellant densities were determined in Dow Corning 200 Fluid, 1.5 centistokes at 25°C. Prior swelling experiments were performed on propellant samples at 71°C, and weight increases of less than 0.19% were observed.

## RESULTS AND DISCUSSION

The viscoelastic spectrum in tension and shear of propellant N-29 is shown in the figures that follow (Figs. 1-8); N-29 is a carboxyl-terminated polybutadiene propellant. A comparison of Figures 1 and 2 reveals almost identical values of the dynamic moduli in tension and shear,  $E' \simeq G'$ , from the rubbery region until about 20°C above  $T_g$ . Both moduli were expected to be different, as was observed by the authors on carbon black-filled rubber, where  $E' \simeq 3G'$ . Each loss tangent curve indicates two distinct maxima, which shift with the frequency along the temperature scale.<sup>1</sup> It is apparent that the second dynamic loss peaks in tension are sharper and more

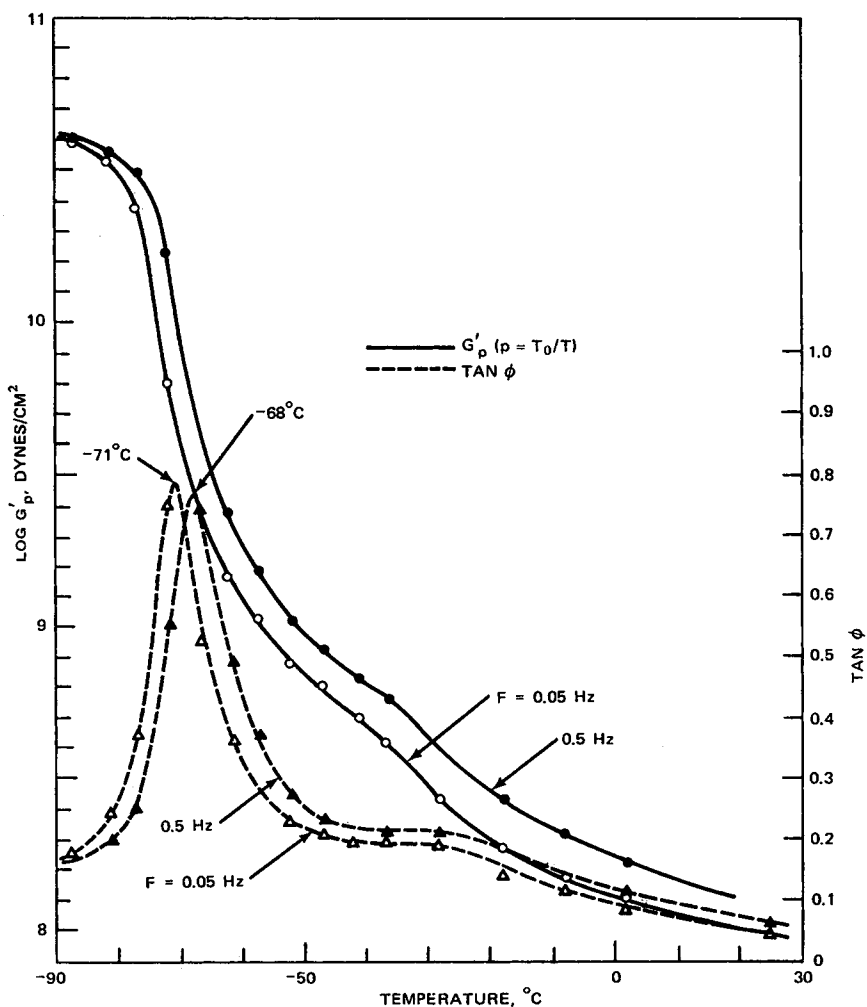


Fig. 1. Dynamic shear properties as functions of frequency and temperature (N-29 propellant).

intense than peaks at the same frequencies in torsion. The different positions of the glass transition peaks occur at different temperatures for the same frequency: the peaks are  $6^{\circ}\text{C}$  higher in tension than in torsion. These observations may be a consequence of the nonuniform and varying shear gradients within the sample under torsion. The deformation in dynamic tension is  $\pm 0.25\%$ , i.e., nearly infinitesimal. The average shear deformation was calculated to be of the same order of magnitude.

It is of interest to note at this point that, for propellant and other highly filled materials,  $E \neq 2(1 + \nu)G$ . The equality is only valid for isotropic, elastic materials undergoing small (infinitesimal) deformations in a homogeneous stress field. In a relatively simple case, the effect of strain-

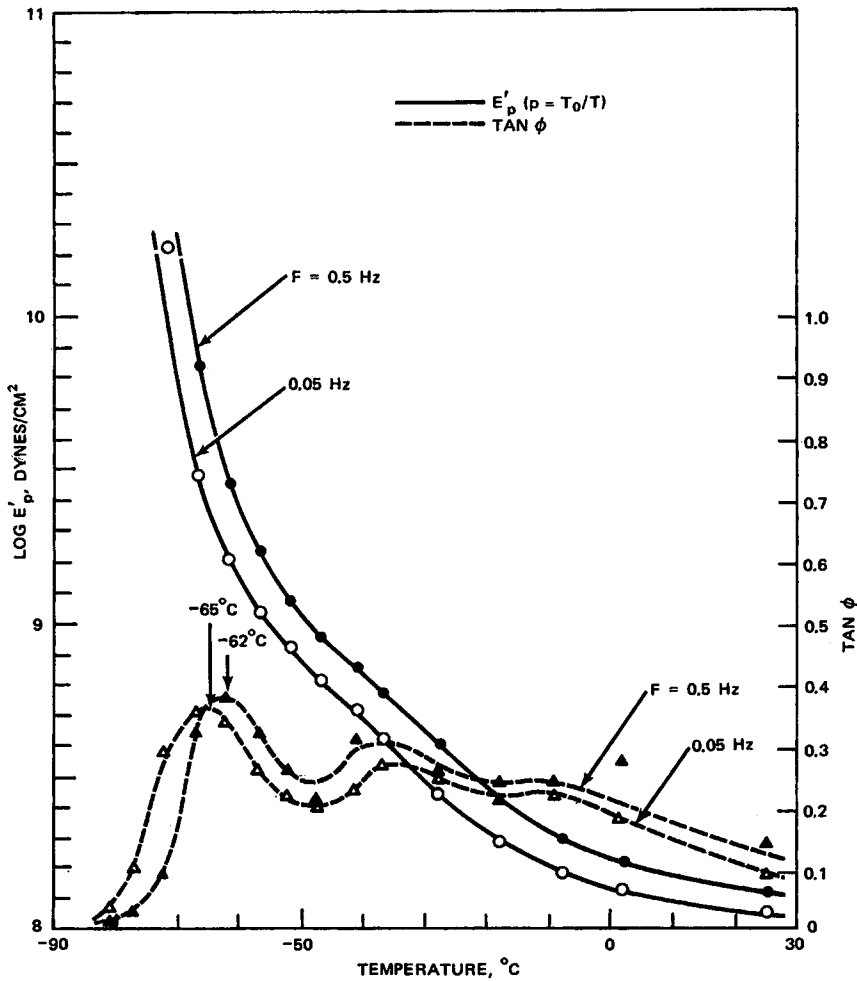


Fig. 2. Dynamic tensile properties as functions of frequency and temperature (N-29 propellant).

induced anisotropy has been determined by Peng and Tschoegl<sup>4</sup> where, using the Valanis-Landel strain energy function, an equation was obtained which approximately accounted for the observed relationship between the superposed dynamic moduli for static strains as large as 6%. For the case of a linear viscoelastic material, Tschoegl<sup>5</sup> has derived a relationship between  $E$  and  $G$  where it is clearly shown than even for rheologically simple, time-dependent materials,  $E \neq 2(1 + \nu)G$ . For the extreme case of high strains of highly filled systems, which are in reality nonlinear viscoelastic and inhomogeneous, no simple relationship between  $E$  and  $G$  exists.

For the small displacements in this paper, the absolute values of the complex dynamic shear modulus,

$$G^* = \sqrt{(G')^2 + (G'')^2}$$

at a constant frequency of 0.5 Hz are shown in Figure 3. The shape of the resulting  $G^*(T)$  curve is dictated primarily by the shape of the  $G'(T)$  curve. It appears that the storage modulus can be used to describe nearly a simple viscoelastic material, while  $G''$  highlights the nonsimple thermorheological

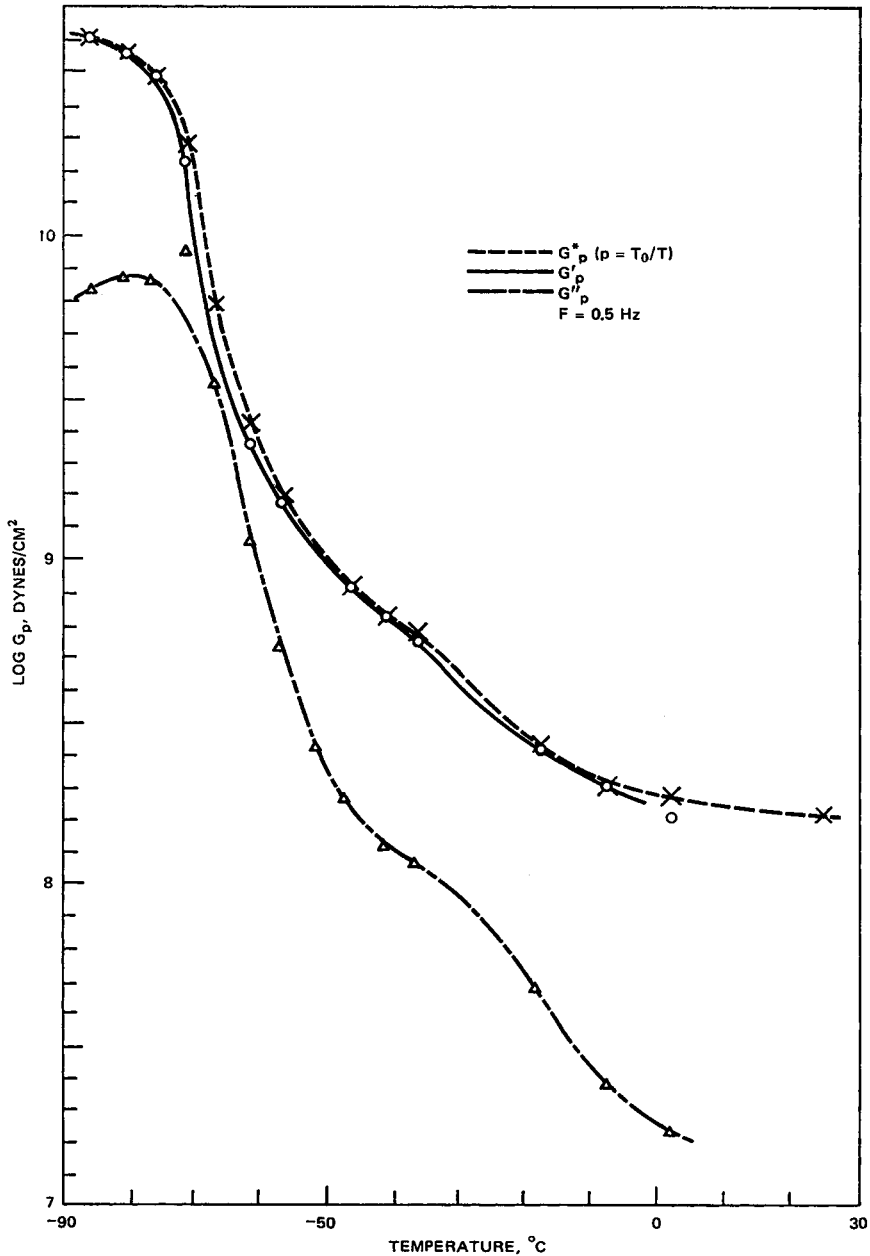


Fig. 3. Complex dynamic moduli vs. temperature (N-29 propellant).

behavior of the propellant. As reported previously,<sup>1</sup> it was discovered that  $G'(T)$  and  $G''(T)$  have different shift factors.

The isotherms for the dynamic tensile and shear moduli as functions of frequency are plotted in Figures 4 and 5. The data, when shifted by superposition of transparencies, shift well, with a slight discontinuity indicated in the region of  $-30^\circ\text{C}$  where the loss tangent curves show a second maximum.

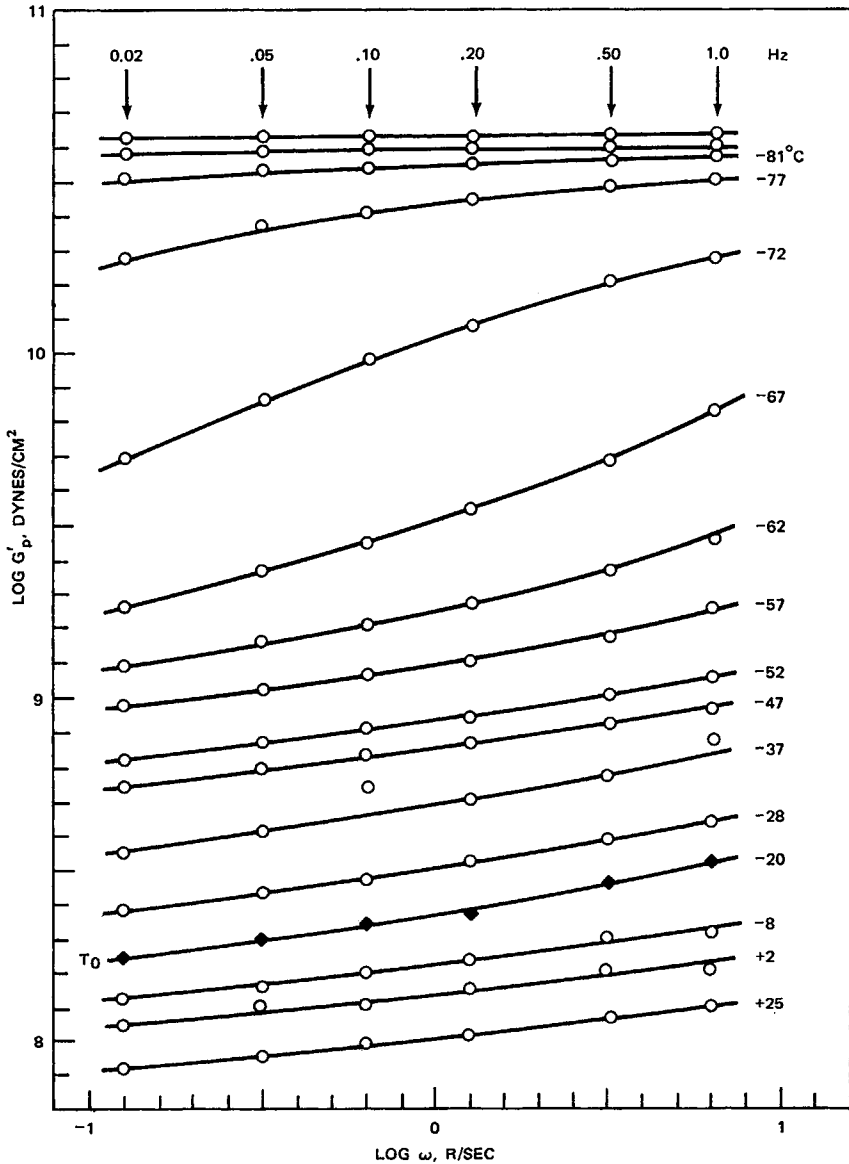


Fig. 4. Temperature-corrected shear moduli as functions of frequency and temperature (N-29 propellant).

The resulting  $a_T$  plots are seen in Figure 6, where it can be observed that, using the same reduced reference temperature, the shift factors appear to nearly coincide for  $G'$  and  $E'$  over the temperature range  $-60^\circ\text{C}$  to about  $-15^\circ\text{C}$ . The data in the room temperature region begin to deviate sharply.

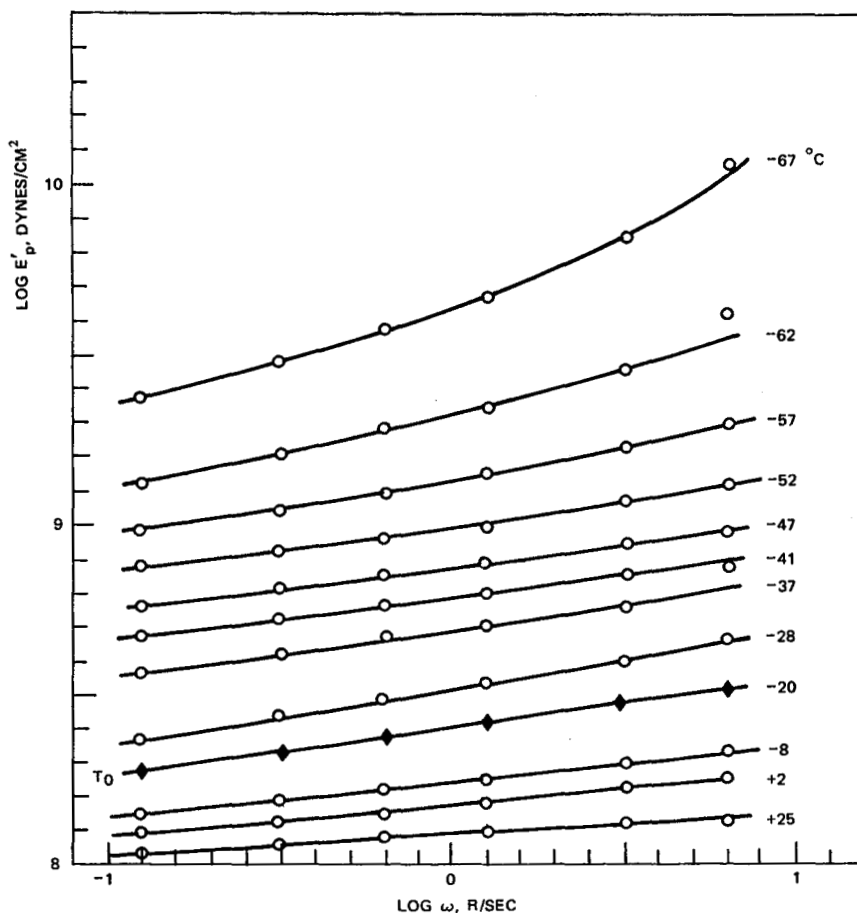


Fig. 5. Temperature-corrected tensile moduli as functions of frequency and temperature (N-29 propellant).

The master plot for the corrected dynamic shear moduli is seen in Figure 7. The overlap of the data at the various temperature ranges is seen to be quite good. A similar plot for the dynamic tensile storage modulus is seen in Figure 8. It is noted that there is a region of reduced temperature where the curve indicates a hump because of the secondary transition.

Comparison of the reduced master curves for dynamic tensile moduli with the dynamic shear moduli indicates that the two curves are nearly superposable until the beginning of the glass transition region.

The effect of dewetting on the shear and tensile properties at constant frequency  $F = 0.5$  Hz is shown in Figure 9.

A freshly machined sample of propellant was placed into the tester, and the dynamic tensile properties over the whole temperature range were determined at small oscillations with an amplitude of  $\Delta L = \pm 0.25\%$  and a

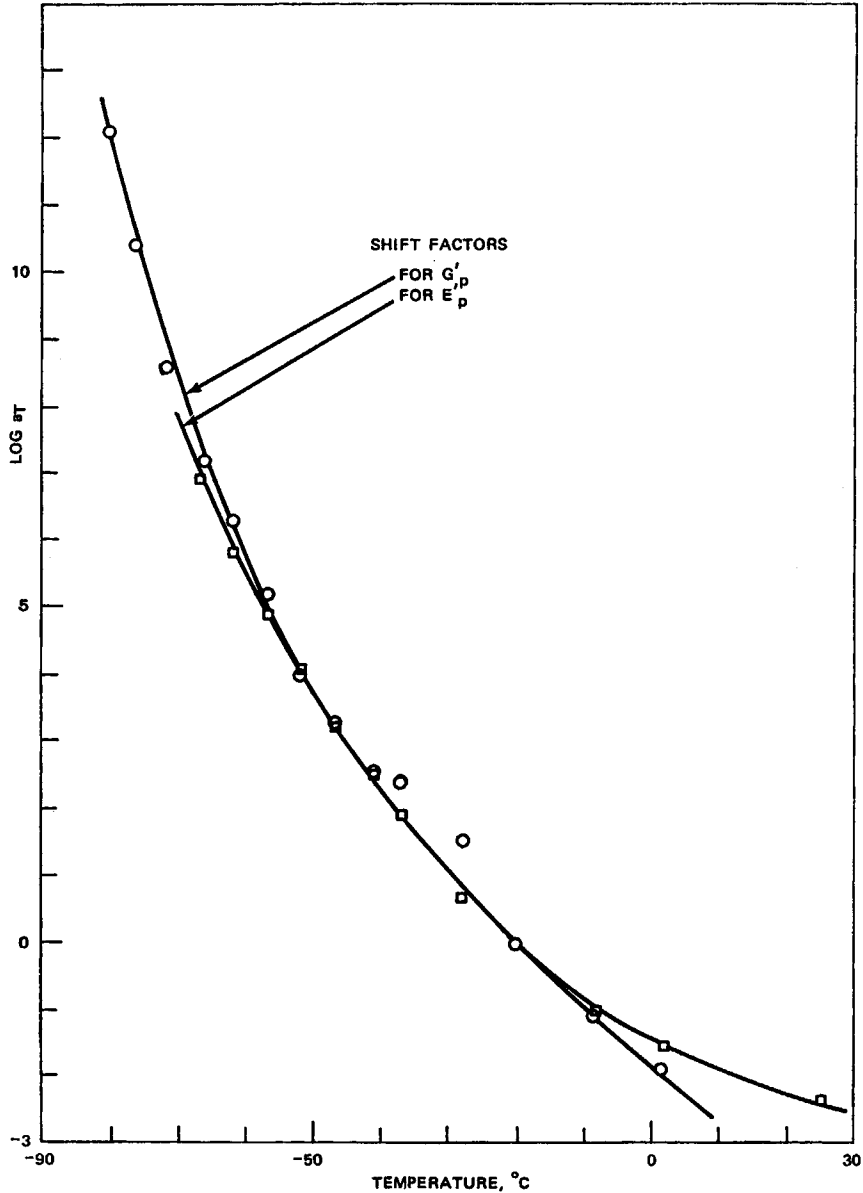


Fig. 6. Time-temperature shift factors for dynamic tensile and shear moduli vs. temperature (N-29 propellant).



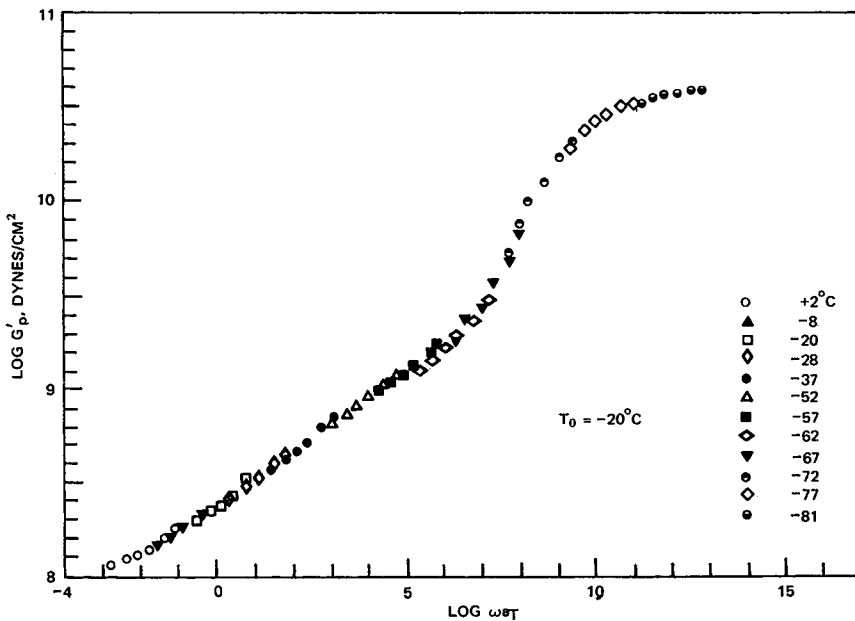


Fig. 7. Reduced master curve for shear modulus of N-29 propellant.

0.5-Hz frequency. The solid curves show the dynamic tensile moduli and loss tangents of an undewetted propellant.

After the same sample had been subjected for 1 hr to a 5.6% tensile cycling at 0.02 Hz, the sample was returned to a zero-strain condition and the dynamic properties were redetermined. The dot-dash curve in Figure 9 was obtained. The sample was then subjected to a larger tensile cycling experiment of 10% strain at 0.013 Hz. After 3 hr, the sample was again returned to zero strain and the dynamic properties were again redetermined, yielding the dashed curve in Figure 9.

In addition to the above data, the dimensions of the propellant were measured after 0, 5.6%, and 10.0% extension cycles. A density of the propellant was measured before beginning the experiment and after the 10.0% cycling experiment. A relative volume increase of  $\Delta V/V_0 = \pm 0.002$  was

TABLE I  
Dewetting Experiment<sup>a</sup>

Strain amplitude, %	Density at zero stress, g/cm <sup>3</sup>	Specific volume at zero stress cm <sup>3</sup> /g	Void concentration $C = \Delta V/V_0$	Tan $\phi$	Lateral strain $\Delta a/a_0$
Theoretical	1.5810	0.6325	0	—	—
0	1.5545	0.6433	0.0171	0.260	0.0259
6.9	1.5533	0.6438	0.0179	0.270	0.0240
10.0	1.5516	0.6445	0.0190	0.285	0.0232

<sup>a</sup>  $V_0$  = Theoretical volume of unstrained propellant.

observed from the change in propellant density. The lateral strain observed during the cycling experiments was found to continually decrease with cycling time.

It should also be noted that a change in modulus occurs as a result of dewetting. The modulus at 23°C changes from  $3.55 \times 10^8$  dynes/cm<sup>2</sup> for the uncycled propellant to  $2.51 \times 10^8$  dynes/cm<sup>2</sup> for the 10% cycled propellant. A further observation can be made that the loss peak observed

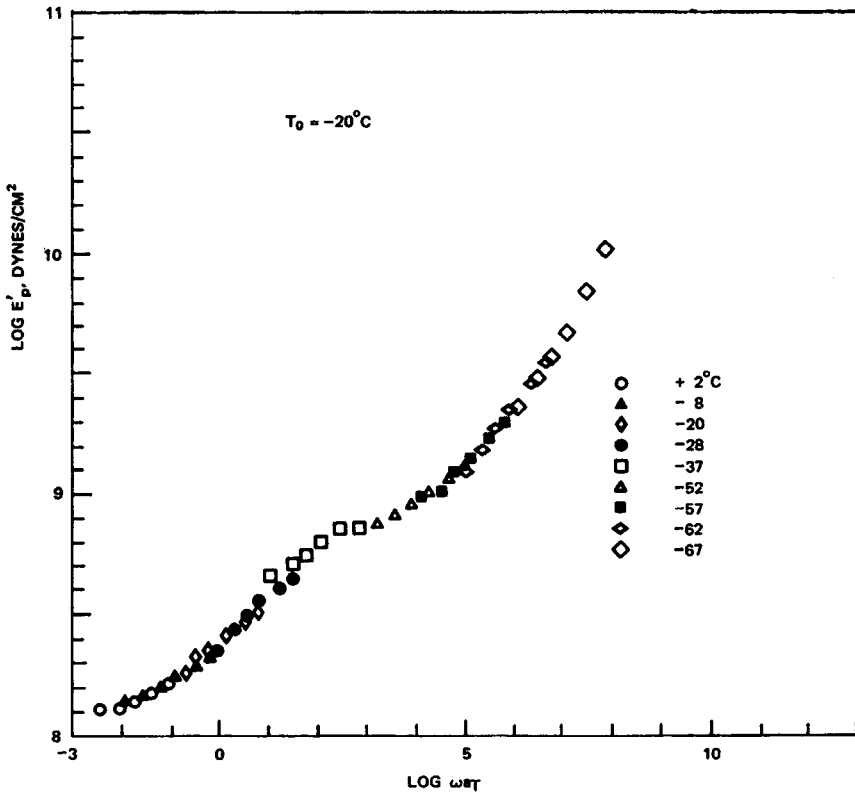


Fig. 8. Reduced master curve for tensile modulus of N-29 propellant.

at  $-23^{\circ}\text{C}$  increases as a function of dewetting. This shows that the  $-23^{\circ}\text{C}$  loss peak is associated with the extent of dewetting. Table I shows the experimental results.

If the dynamic loss peak transitions are treated like the absorbances in optical spectroscopy, attempts can be made to obtain a relation between the concentration of microstructural grouping and the dynamic loss. Equation (1) is an attempt to extend Beer-Lambert's law to mechanical spectroscopy:

$$\frac{\tan\phi}{\tan\phi_0} = \exp(-kC) \quad (1)$$

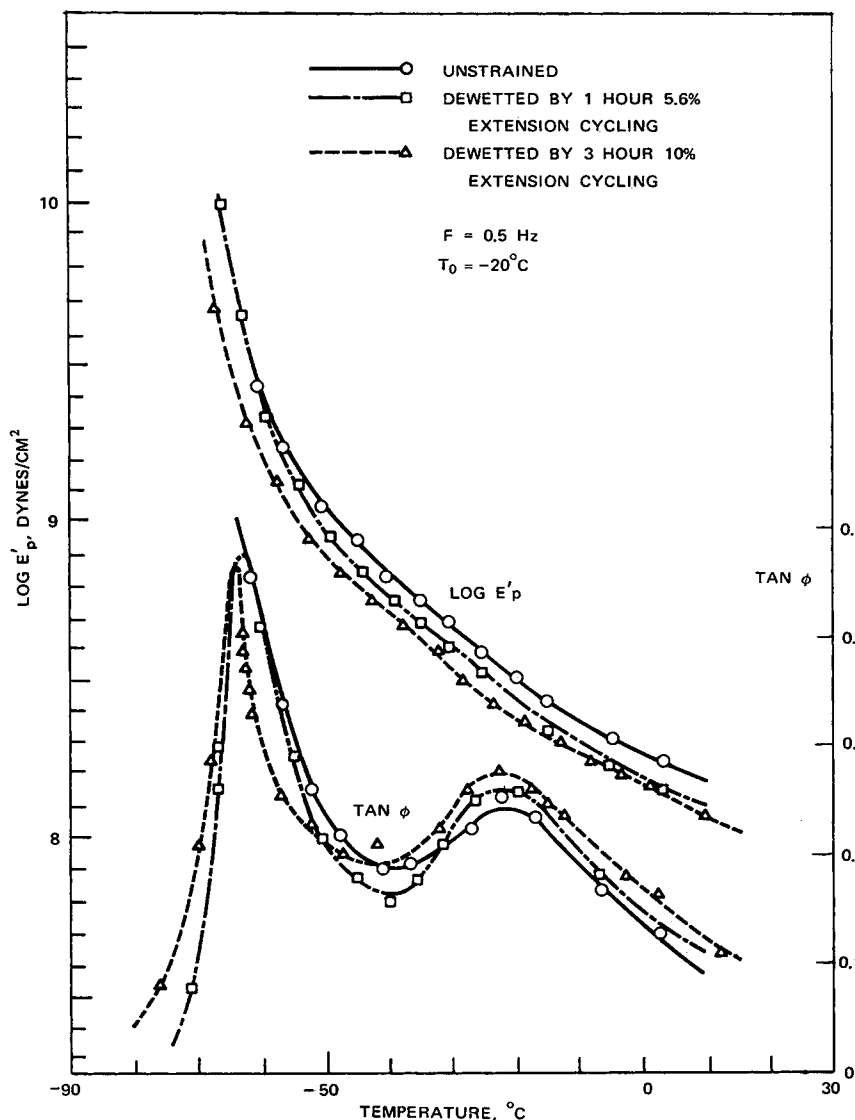


Fig. 9. Effect of dewetting on the dynamic tensile properties of propellant C55-A.

where  $\tan\phi$  refers to the dynamic loss associated with the void concentration  $C$ ,  $\tan\phi_0$  is the dynamic loss associated with the zero void concentration, and  $k$  is the analog of the Beer-Lambert's constant.

If the increase in void concentration and the associated increase in the dynamic loss are known, then the constant  $k$  can be evaluated from equation (2):

$$\log_e \left( \frac{\tan\phi_1}{\tan\phi_2} \right) = -k\Delta C. \tag{2}$$

On the basis of the data in Figure 9 and the assumption of a linear relationship between  $\phi$  and  $C$ , one can calculate  $k = 49$ , where the concentration is expressed in terms of volume fraction of voids. If the assumptions in this treatment are correct, the void concentration of the unstrained propellant is 0.0172 volume fraction. From calculation of the theoretical density (the density calculated from the propellant composition) and the measured density of 1.5545 g/cm<sup>3</sup> for the unstrained sample, one can calculate an initial void concentration of 0.017.

### CONCLUSIONS

The following conclusions are based on data presented in this paper:

1. The corresponding dynamic moduli in tension and shear of propellants are found to have almost identical values, instead of the expected ratio of  $E'/G' \sim 3$ .
2. The loss tangent curves from dynamic tensile measurements are more sensitive in showing maxima peaks than similar curves from torsional measurements.
3. The WLF shift factors of  $E'$  and  $G'$  are nearly identical from  $-15^\circ$  to  $-60^\circ\text{C}$ .
4. The transition of the propellant at  $-23^\circ\text{C}$  is related to the degree of dewetting.
5. The glass transition peaks of the loss tangents in tension and torsion occur at different temperatures.
6. There is some indication that the dynamic loss peaks can be treated similarly to optical spectroscopy, where the peak heights are related to microstructural contributors to the loss.

### References

1. A. Adicoff and A. Lepie, *Effect on Tensile Strain on the Use of the WLF-Equation*, ICRPG Manual, 7th Meeting, November 1968.
2. A. Lepie and A. Adicoff, *Rev. Sci. Instrum.*, **38**, (11), 1967.
3. A. Lepie, *Rev. Sci. Instrum.*, **40**, (8), 1004 (1969).
4. T. J. Peng, and N. W. Tschoegl, paper presented at the Winter Meeting, Rheology Society, California Institute of Technology, Pasadena, Calif., Feb. 2-4, 1970.
5. N. W. Tschoegl, private communication, 1969.

Received January 25, 1971

Revised August 2, 1971